第29卷第5期
2010年10月

红外与毫米波学报
J. Infrared Millim. Waves

Vol. 29, No. 5
October, 2010

文章编号:1001 - 9014(2010)05 - 0321 - 04

RESONATE MODES IN PHOTOACOUSTIC CELL FOR GAS SENSING

ZHANG Xiao-Jun[1,2], ZHANG Yong-Gang[1*]

(1. State Key Laboratory of Functional Materials for Informatics, Shanghai Institute of Microsystem and Information Technology, Chinese Academy of Sciences, Shanghai 20050, China;
2. Graduate School, Chinese Academy of Sciences, Beijing 100039, China)

Abstract: A cylinder shape photoacoustic (PA) cell has been designed and fabricated for mid-infrared laser photoacoustic spectroscopy (MIR-PAS) gas sensing application. A complete modeling of the acoustic signal transmission and detection in the PA cell using FEM have been performed to simulate its characteristics and compared systemtically with the measured data. Results show that the second longitudinal mode of the PA cell has the highest resonance amplitude around 4.2 KHz with moderate Q value, so this mode is quite suitable for MIR-PAS gas sensing purpose.

Key words: Photoacoustic spectroscopy; gas sensing; resonance frequency; finite element method
CLC number: TB4 **Document**: A

红外激光光声光谱气体传感谐振腔分析

张晓钧[1,2], 张永刚[1]

(1. 中国科学院上海微系统与信息技术研究所 信息功能材料国家重点实验室, 上海 200050;
2. 中国科学院研究生院, 北京 100039)

摘要: 设计制作了适合中红外激光光声光谱气体检测用的圆柱形光声腔, 采用有限元法对其声信号的传输和探测进行了模拟分析并与实际测量结果进行了系统的比较. 结果表明此光声腔中的二阶纵模在4.2KHz附近具有最大的共振幅度和适中的Q值, 十分适合中红外光声光谱气体传感应用.

关 键 词: 光声光谱; 气体传感; 共振频率; 有限元方法

Introduction

The photoacoustic detection is based on photoacoustic effect discovered by Bell in the 1880s[1,2]. The energy of incident light absorbed by the molecules of gases energy of light absorbed molecules is essentially transferred into kinetic energy of the surrounding molecules via collisions. This induces a local pressure change in the absorbing gas. If the light source is modulated, an acoustic wave is generated that can be detected by a sensitive acoustic sensor such as microphone. Usually the oscillation is in the sound frequency range, so this method is called photoacoustic spectroscopy (PAS). Figure 1 shows the principle of PAS, and Fig. 2 shows the schematic of a PAS gas sensor.

It is known that dominant absorption lines of the gases are in infrared, especially the mid-infrared (MIR) band of 2 ~ 25μm, corresponding to the frequencies of molecular vibrations of the gases. Therefore the progresses in mid-infrared lasers [3~5] accelerates the development of MIR-PAS so rapidly, which is a powerful technique for trace-level gas sensing because it combines high sensitivity and the ruggedness required for field deployable instrumentation and have

Received date: 2009 - 09 - 01, **revised date**: 2010 - 03 - 19 **收稿日期**:2009 - 09 - 01, **修回日期**:2010 - 03 - 19
Foudantion item: NSFC(60876034); 973(2006CB604); CAS Innovation(KGCX2-YW-121)
Biography: Zhang Xiao-jun, (1983-), male, Jiangsu, China. Ph. D. candidate, research on application of optoelectronic devices.
* **Corresponding author**: E-mail: ygzhang@mail.sim.ac.cn.

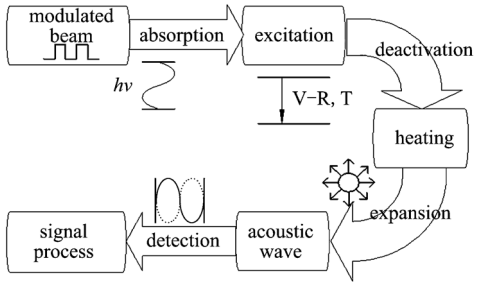

Fig. 1 Principle of PAS
图1 光声光谱原理图

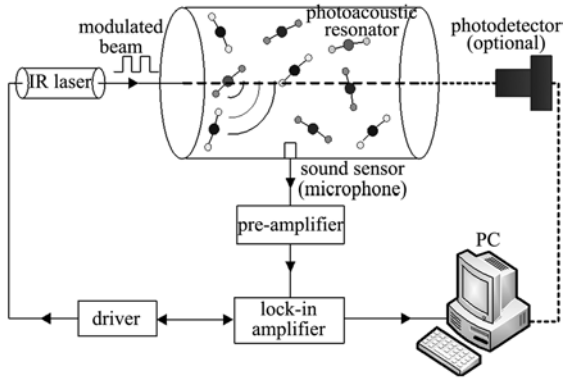

Fig. 2 Schematic of a PAS gas sensor
图2 光声光谱气体传感器示意图

already found many applications in the field of trace gas sensing [6~8]. The MIR-PAS has attracted much of our interest which can help us achieve new detection limits with the base of MIR laser spectroscopy trace gas sensing these years [9~11].

2 Acoustic theory of PA cells

It has been demonstrated that using a cavity as an acoustic amplifier of the sound signal was very important in PAS. Also, the cavity has eigenmodes with certain resonance frequencies at which the stronger sound signal could be observed effectively. So the acoustic parameters are greatly concerned.

The sensitivity of a photoacoustic sensor strongly depends on the geometry of the photoacoustic cell. It can be considerably improved by taking the advantage of acoustical cell resonances, i.e., the laser radiation is modulated at a frequency match to one of the resonance frequencies. Cavities of cylindrical shape as photoacoustic cells have been well investigated; many kinds of PAS cells with unconventional shapes have been designed and developed in recent years [12]. In order to design a PAS system, it is important to understand the pressure distribution in the PAS cell precisely. Therefore, a systematically acoustics analysis of the PA cell should be performed with simulation and experiment, respectively, and the resonance frequencies can be obtained. The pressure amplitudes at the position of microphone can also be obtained which are proportional to the PA signal.

In a photoacoustic cell, the Helmholtz equation can be derived for the sound pressure:

$$\vec{\nabla}^2 p(\vec{r},\omega) + k^2 p(\vec{r},\omega) = i\omega \frac{\gamma - 1}{c^2} H(\vec{r},\omega) \quad , (1)$$

where $k = \omega/c$, c is the sound velocity of the gas, γ denotes the ratio of the specific heat at constant pressure c_p to the specific heat at constant volume c_V, and H is the heat density absorbed by the gas from light which can be calculated from the relation $H = \alpha I$ where I is the intensity of the electromagnetic field and α is the absorption coefficient[13].

Assuming that the walls of the PA cell are sound hard which leads to the boundary condition $\partial p/\partial n = 0$ (here n is normal direction), the acoustic eigenfrequencies of a closed cavity are the solutions of the wave equation

$$\vec{\nabla}^2 p + k^2 p = 0 \quad , \qquad (2)$$

By solving the equation above, the dimensionless eigenmode distribution function of a cylindrical resonator could be given as

$$\begin{aligned} p(\mathrm{r}) &= p_{jmq}(r,\varphi,z) \\ &= J_m(\pi\alpha_{jm})\cos(m\varphi)\cos(q\pi z/L) \end{aligned} \qquad (3)$$

Where L is the length of the cylinder, the jmq indices refer to the eigenvalues of the radial, azimuthal, and longitudinal modes respectively, and α_{jm} is the jth zero of the derivative of the m_{th} Bessel function divided by π.

More detailed theories about optimum design of PA cells can be found in ref [14].

3 Design and fabrication of a MIR-PAS cell

To make a cell for MIR-PAS, its shape and size should be carefully considered. First, for a convention-

al cylinder cell, the ratio L/R of cavity length L over radius R should be high enough for effective acoustic resonance. Second, a compact cell should be more favorable for its small sample volume, at the same time a moderate resonance frequency is expected. Furthermore, an overall tradeoff is often needed for the feasibility of fabrication and compatibility to other cell components such as windows, acoustic sensor, gas inlet and outlet, and so on. Based on above considerations, a cylinder shape MIR-PAS cell with cavity length of $L = 80$mm and radius $R = 9$mm is designed as shown in Fig. 3. The sample volume of this cell is about 20cm^3. A real cell with the same size is fabricated with brass. A low-cost electret microphone with 6mm in diameter is used as the acoustic sensor installed on the position shown in Fig. 3 with a 4mm opening to the cavity. The ends of the cavity are enclosed by two IR optical windows (one for laser entrance and the other is optional for light monitor) made of KRS-5 crystals, which are sealed by O rings. The KRS-5 is a well known nondeliquescent optical window material transparent from 0.5 to 40μm, covering both the NIR and MIR bands, quite suitable for MIR-PAS applications. Other two small openings 2mm in diameter located asymmetrically on the cavity wall, which are connected to two valves, were used as sample gas inlet and outlet.

4　Evaluation of the PA cell and discussions

In the simulation the cell is supposed to fulfill with air under atmospheric conditions ($T = 300$K, $p = 1$atm). The speed of sound c is 343m/s. The microphone used to detect the acoustic signal is supposed to be installed on the middle of the cell wall. Finite element method (FEM) is used to calculate the eigenmodes and the contribution of sound pressure in the PA cell. The first four longitudinal modes ($f < 10$kHz) are calculated as shown in Fig. 4, the mode frequencies are listed in Table 1. Notice that in the calculation second boundary condition ($\partial p/\partial n = 0$) is used based on the practical configurations. These eigenmodes (as shown in Fig. 4) are different from those with first boundary condition ($p = 0$ at ends).

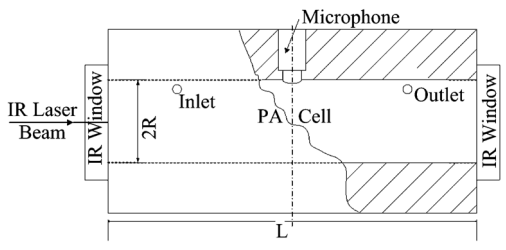

Fig. 3　Schematic of the IR-PAS cavity
图 3　红外激光光声光谱气体腔示意图

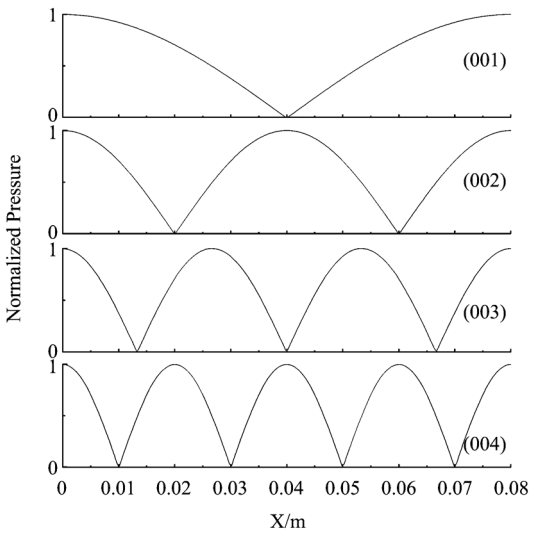

Fig. 4　The results of eigenmodes in the condition of second boundary
图 4　第二类边界条件下的本征模式示意图

Based on the calculated eigenmodes, resonate response is simulated under hard wall assumption. In the simulation a specified point in the cell is set as a sound source to excite more eigenmode, the sound pressure at microphone position is recorded as shown in Fig. 5 (b). The simulated resonance frequencies are consistent with the eigenmodes precisely. From Fig. 5 (b) a sharp resonance with very high Q value could be observed, while in practice the sound media with bulk viscosity in conjunction with other loss effects influ-

Table 1　Simulated and measured resonate frequencies of longitudinal modes of the PA cavity
表 1　光声腔共振频率的模拟与测量值

Frequency	Simulation	Measurement
f_{001} (Hz)	2143.77	2346 ($Q_{001} \approx 4.67$)
f_{002} (Hz)	4287.57	4235 ($Q_{002} \approx 23.79$)
f_{003} (Hz)	6431.61	6285 ($Q_{003} \approx 25.76$)
f_{004} (Hz)	8576.65	8352 ($Q_{004} \approx 29.10$)

ences the transmission of sound and depress the Q values notably, so the damping effects should be considered. Therefore a damping coefficient, which is given by the complex wave number and the complex impedance, was introduced into resonate response simulation as shown in Fig. 5(c). It can be seen that, the profile becomes flat with much lower peak values, the resonance frequencies keeps almost the same whereas the halfwidth values of the resonance profile increase notably, that makes the Q values decrease dramatically.

If transmission line theory, four-terminal network or other methods can be introduced to the simulation, they may provide the more accurate simulation results, which would be a great help for our further experiment.

To evaluate the real cell experimentally, acoustic measurements was performed. In the measurements one KRS-5 window is replaced by a mini loudspeaker to excite sound waves in the cell. The loudspeaker is driven by a sine wave generator. The sound signal detected by the electret micrphone are feed into a SR830 lock-in amplifier. In the experiments all the instruments and frequency scan are controlled via GPIB by a computer. The frequency properties of the loudspeaker and microphone were calibrated before the experiments.

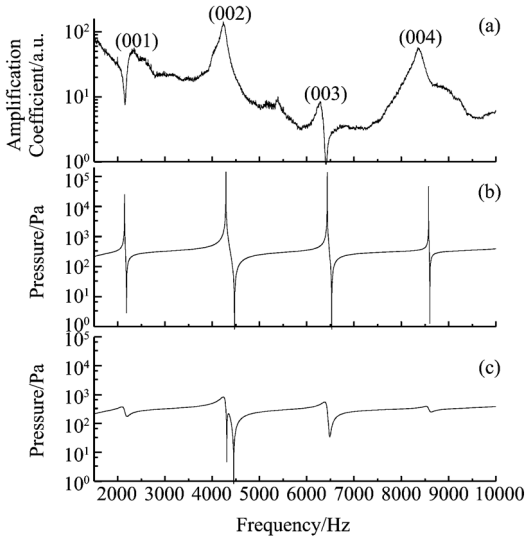

Fig. 5 Simulated and measured characteristics of the PA cavity (a) Measured frequency dependent amplification coefficient of the PA cell (b) and (c) Simulated resonance response for the cell without and with damping coefficient

图5 光声腔特性的模拟与实测结果 (a)实测光声腔的放大系数与频率的关系 (b)和(c)分别是不考虑和考虑衰减系数时光声腔的共振频率响应模拟结果

The measured resonate response of the cell is shown in Fig. 5 (a). This response curve shows the amplification effect of the PA cell at different frequencies, and four resonance frequencies, which are almost in accordance with the simulation results, could be observed. The resonance frequencies and educed Q values from Fig. 5 (a) are also listed in Table 1. A small offset between the measured response peak and the simulated resonance frequencies could be found, which may come from the errors of the size dimension, simulation parameters as well as the influence of small openings on the cavity wall. Notice that the FEM simulations are performed under ideal conditions, a small shift of the measured resonance frequency with the simulation is reasonable.

As shown in Fig. 4, the current position of microphone is less suitable for the detection of odd eigenmodes such as 001 and 003 than the even eigenmodes, and much lower amplitude could be observed in those modes from the measured results. In practice the loudspeaker could be considered as a plane acoustic source, so in this plane many exciting points could be found which can excite the odd longitudinal modes although their amplitude is limited. This phenomenon has been confirmed by simulation as shown in Fig. 6.

From the simulated and measured results it could be inferred that, for the PA cell in this configuration the 002 even longitudinal mode has the highest resonance amplitude with moderate Q value, also the resonance frequency around 4.2 KHz is quite suitable for using conventional microphone as the acoustic sensor. Also at this modulation frequency range the electronics and signal processing becomes easier. Furthermore, when IR laser beam was used to excite the sound wave in the PA cell along the longitudinal axis, this mode should also be the most effective one; therefore this mode should be most favorable for PAS gas sensing applications.

5 Conclusion

In conclusion, a cylinder shape PA cell with about 20 cm^3 sample volume has been designed and fabricated, complete modeling of the acoustic signal trans-

(下转341页)

cadmium telluride[J]. *J Appl Phys.*,1991,**69**(7):3849—3852.
[8] Dawar A L, Savita Roy, Mall R P, *et al.* Effect of laser irradiation on structural, electrical, and optical properties of p-mercury cadmium telluride[J]. *J App*l *Phys.*,1991,**70**(7):3516—3520.
[9] Zha F X, Zhou S M, Ma H L, *et al.* Laser drilling induced electrical type inversion in vacancy-doped p-type HgCdTe [J]. *Appl. Phys. Lett.*,2008,**93**:151113.
[10] Zha F X, Li M S, Shao J, *et al.* Femtosecond laser-drilling induced HgCdTe Photodiodes[J]. *OPTICS LETTERS*, 2010,**35**(7):971.
[11] Siliquini J F, Dell J M, Musca C A, *et al.* Scanning laser microscopy of reactive ion etching induced n-type conversion in vacancy-doped p-type HgCdTe[J]. *Appl. Phys. Lett.*,1997,**70**:3443.
[12] YE Zhen-Hua, HU Xiao-Ning, CAI Wei-Ying, *et al.* Application of laser beam induced current for technology detecting of HgCdTe two-color detector[J]. *J. Infrared Millim. Waves*(叶振华,胡晓宁,蔡炜颖,等. 激光束诱导电流在 HgCdTe 双色探测器工艺检测中的应用. **红外与毫米波学报**),2005,**24**(6):459—462.
[13] CAI Wei-Ying. Laser beam current induce technology and characterization of semiconduct[J]. *Infrared*(蔡炜颖. LBIC 技术与半导体材料特性的表征. **红外**),2000,**9**:12—14.

(上接 324 页)

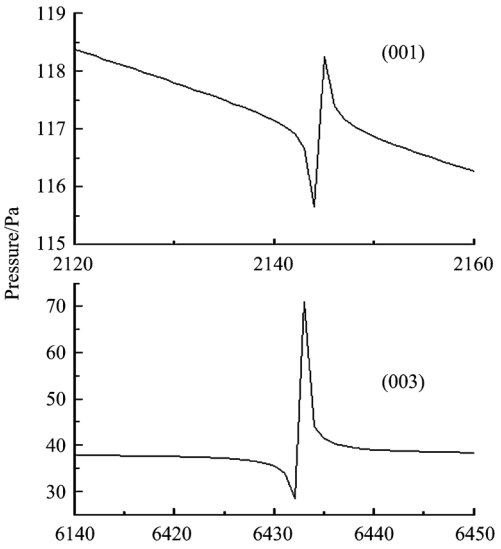

Fig. 6　The simulated odd harmonic response of the PA cavity with certain exiting point in the loudspeaker plane
图 6　光声腔在扬声器平面上特定点激发产生的奇次谐波响应的模拟结果

mission and detection in the PA cell using FEM have been performed to simulate its features and compared with the measured data. Results show that the second longitudinal mode of the PA cell has the highest resonance amplitude around 4.2 KHz with moderate Q value, so this mode is quite suitable for MIR-PAS gas sensing purpose.

REFERENCES

[1] BELL A G. On the production and reproduction of sound by light[J]. *Am. J. Sci.*,1880,XX:305—324.
[2] BELL A G. Upon the production of sound by radiant energy [J]. *Phil. Mag. J. Sci.*,1881,XI:510—528.
[3] ZHANG Yong-gang, ZHENG Yan-Lan, LIN Chun, *et al.* Continuous wave performance and tunability of MBE grown 2.1μm InGaAsSb /AlGaAsSb MQW lasers[J]. *Chin. Phys. Lett.*,2006,**23**(8):2262.
[4] BAI Y, SLIVKEN S, DARVISH S R, *et al.* Room temperature continuous wave operation of quantum cascade lasers with 12.5% wall plug efficiency[J]. *Appl. Phys. Lett.*, 2008,**93**,2.
[5] LYAKH A, PFLUGL C., Diehl L, *et al.* 1.6 W high wall plug efficiency, continuous-wave room temperature quantum cascade laser emitting at 4.6μm[J]. *Appl. Phys. Lett.*, 2008,**92**,11.
[6] FILHO M B, DA Silva M G, STHEL M S, *et al.* Ammonia detection by using quantum-cascade laser photoacoustic spectroscopy[J]. *Applied Optics*, 2006, **45**(20): 4966—4971.
[7] GROSSEL A, ZENINARI V, JOLY L, *et al.* Photoacoustic detection of nitric oxide with a Helmholtz resonant quantum cascade laser sensor[J]. *Infrared Phys. & Tech.*,2007,**51**(2):95—101.
[8] MUKHERJEE A, DUNAYEVSKIY I, PRASANNA M, *et al.* Sub-parts-per-billion level detection of dimethyl methyl phosphonate (DMMP) by quantum cascade laser photoacoustic spectroscopy[J]. *Applied Optics*, 2008, **47**(10): 1543—1548.
[9] ZHANG Yong-gang, XU Gang-Yi, LI Ai-Zhen, *et al.* Pulse wavelength scan of room-temperature mid-infrared distributed feedback quantum cascade lasers for N_2O gas detection [J]. *Chin. Phys. Lett.*,2006,**23**(7):1780.
[10] ZHANG Yong-gang, ZHANG Xiao-Jun, ZHU Xiang-Rong, *et al.* Tunable diode laser absorption spectroscopy detection of N_2O at 2.1μm using antimonide laser and InGaAs photodiode[J]. *Chin. Phys. Lett.*,2007,**24**(8): 2301.
[11] ZHANG Yong-gang, GU Yi, ZHANG Xiao-Jun, *et al.* Gas sensor using a robust approach under time multiplexing scheme with a twin laser chip for absorption and reference [J]. *Chin. Phys. Lett.*,2008,**25**(9):3246.
[12] WOLFF M, GRONINGA H G, BAUMANN B, *et al.* Resonance Investigations using PAS and FEM[J]. *Acta Acustica*,2005,**91**(Suppl. 1):99.
[13] KREUZER L B, The physics of signal generation and detection, *Optoacoustic Spectroscopy and Detection*, Pao, Y.-H. (Ed.)[M]. Academic:London,1-25 (1977).
[14] ANDRAS Miklos, PETER Hess, ZOLTAN Bozoki. Application of acoustic resonators in photoacoustic trace gas analysis and metrology[J]. *Review of Scientific Instruments*,2001,**72**(4):1937—1955.